

Properties of a pilot sample of blue compact dwarf galaxies at intermediate redshifts located in the Hubble Ultra Deep Field

Lucía Rodríguez-Muñoz¹, Jesús Gallego¹, Armando Gil de Paz¹,
Pablo G. Pérez-González¹, Guillermo Barro¹, Víctor Villar¹, and
Jaime Zamorano¹

¹ Departamento de Astrofísica y C.C. de la Atmósfera, Facultad de C.C. Físicas,
Universidad Complutense de Madrid, C.P. 28040 Madrid, Spain

Abstract

We present the analysis of the photometric and spectroscopic properties of a pilot sample of spectroscopically-confirmed intermediate-redshift blue compact dwarf galaxies (BCDs) located in the Hubble Ultra Deep Field. We found that applying the classic BCD definition, we recover a mix of galaxies with a wide range of star-forming activity, metallicity and morphologies.

1 Introduction

Dwarf galaxies still remain as one of the most puzzling components of the universe, since, due to their low luminosity, it is hard to build complete samples of them beyond the bounds of the local universe. Among dwarfs, the so called Blue Compact Dwarfs were defined by [16] as those characterized by low luminosities ($B > -18^1$, strong emission lines, and optical sizes smaller than 1 kpc. These galaxies possess high-surface-brightness nucleus with strong emission lines, due to the intense burst of star formation they undergo, that allow the measurement of redshifts and physical conditions. When observed at low redshifts, BCDs show also an underlying stellar population that trace their star formation history. Deep images taken by ACS/HST make the study of this low luminosity component achievable when the look back time is long enough so that the stellar populations are young enough to allow accurate estimations of their ages and determination of star formation histories [6].

¹We adopt a concordance cosmology: $H_0 = 70 \text{ km s}^{-1} \text{ Mpc}^{-1}$, $\Omega_M = 0.3$, $\Omega_\Lambda = 0.7$.

2 Sample

The selection was carried out using the HST/ACS Ultra Deep Field v.1.0 source catalog released by the Space Telescope Science Institute on March 9th 2004 [2], as a MAST High Level Science Product ² supplemented by photometric redshifts obtained by COMBO-17 [19], ground-based spectroscopic redshifts, obtained by the DEEP2 [9], K20 [12], and VIRMOS-VLT Deep Survey (VVDS [17, 18]) and rest-frame B -band absolute magnitudes, rest frame colors $(B - V)_0$ and surface brightness within the effective radius, $\mu_{\text{eff},B,0}$, computed for available magnitudes and redshifts. In order to identify a sample of BCDs, the selection criteria established were based on the properties that characterize these objects in the local Universe [16, 5]: $M_{B,0} > -18.5$ mag, $(B - V)_0 < 0.6$ mag, and $\mu_{\text{eff},B,0} < 23$ mag arcsec⁻². The redshift range considered was $0.2 < z < 1$. The lower limit was determined by the lower redshift for which the colors showed typically by the underlying stellar population of the galaxies are still sensitive to variations in age, and the higher limit was given by the redshift at which the typical surface-brightness of these kind of objects falls below the UDF sensitivity limits.

Only 9 out of the 132 candidates that matched the selection criteria, had spectroscopic redshift available, so a spectroscopic survey of BCD candidates was carried out using the Magellan Telescopes. The final sample of spectroscopically-confirmed intermediate-redshift BCDs was made up of 15 galaxies. The images of some of them are shown in Fig. 1.

3 Photometric properties

Despite the fact that the 15 galaxies have been selected by the same criteria we find noticeable differences between the BCDs in the sample as can be seen in the subsample shown in Fig. 1. The morphology of the galaxies varies from compact (HUDF0703, HUDF5399, HUDF9088) to irregular (HUDF2215), and even some disk-like objects are found. Only 3 of them display any evidence of interaction (such is the case of HUDF7737 and HUDF9088, that seem to be interacting to each other). All of them show $(B - V)_0$ colors between 0.25 and 0.53 and effective radius between 0.56 and 2.52 kpc. These values are consistent with compact galaxies at different redshifts studied by [14] and [7]. It's worth mentioning that the sample shows a dichotomy in their photometric properties as two different groups can be identified. One of them characterized by properties matching those representative of local HII-like star-forming galaxies, less evolved objects in which the star formation burst dominates the luminosity of the galaxy (UCM Survey [4]), and another one showing properties more similar to those of more evolved local disk-like star-forming galaxies (UCM Survey [4]), whose star-forming activity does not dominate their total luminosity. All these objects are extremely faint and difficult to observe, with apparent magnitudes in the I band around 25 mag.

²The v.1.0 HST/ACS Ultra Deep Field catalogs can be found at <ftp://archive.stsci.edu/pub/hlsp/udf/acs-wfc/>

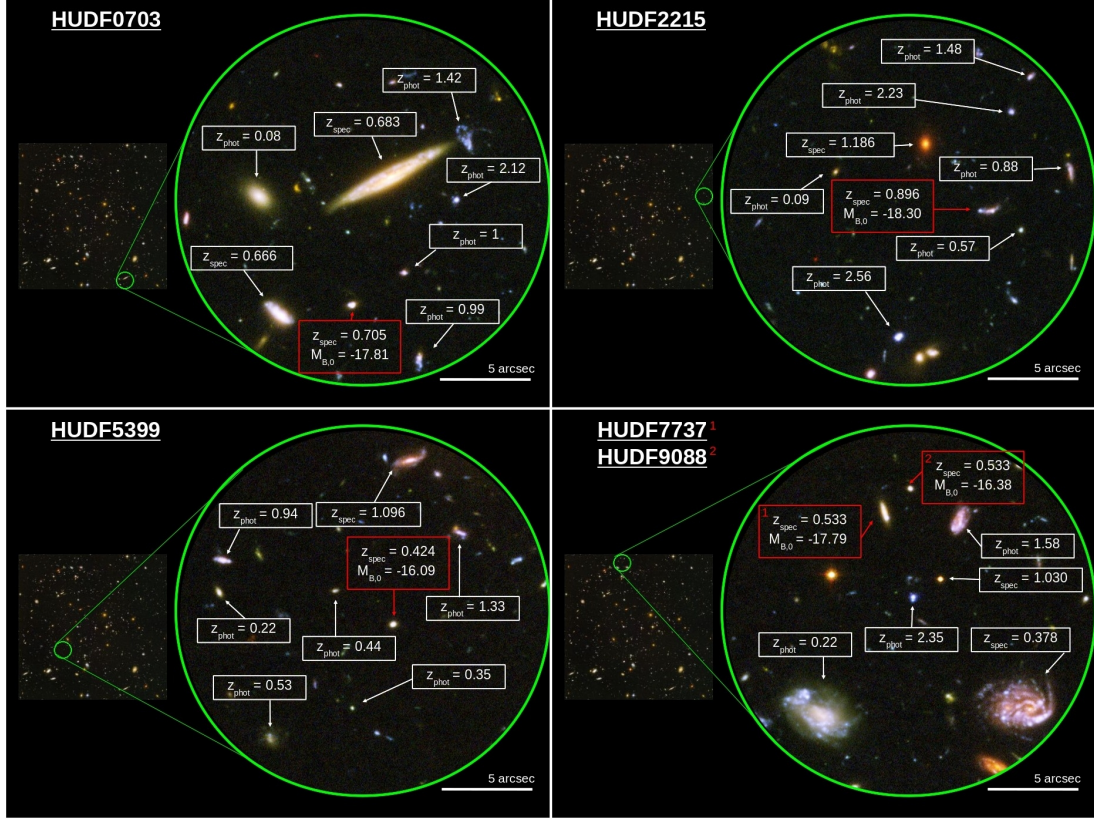


Figure 1: Sub-sample of BCDs. Images extracted from the UDF Skywalker [8]. Photometric redshifts obtained by COMBO-17 [19], and spectroscopic redshifts from our Magellan data and DEEP2 [9] only for HUDF7737. North is up-left, 45 deg.

4 Spectroscopic properties

There were only 14 spectra available to work with and 12 of them were not flux calibrated. The spectral features identified in most of the galaxies were emission lines such as $[\text{OII}]\lambda\lambda 3726, 3729 \text{ \AA}$, $\text{H}\beta$, $[\text{OIII}]\lambda 4959 \text{ \AA}$, and $[\text{OIII}]\lambda 5007 \text{ \AA}$. See Fig. 2.

Assuming the flat shape of the spectra and the low contribution of the continuum we estimate the excitation of the BCDs using the $[\text{OIII}]\lambda 5007/\text{H}\beta$ ratio. Again we find a dichotomy in the physical conditions of the galaxies, as we clearly identify two groups of objects connected by an overlapping region. The group corresponding to those galaxies similar to the local HII-like star-forming galaxies reaches higher values of excitation and lower metallicity ($Z \sim 0.4 Z_{\odot}$) than those similar to the local disk-like star-forming galaxies ($Z \sim 0.8 Z_{\odot}$).

We also measured the velocity dispersion of the galaxies, which had spectra with enough resolution (only 5 objects), and then, we estimated the values of their dynamical masses. The results appear in Fig. 3 (left), where we can see that masses of the BCDs vary between 10^8

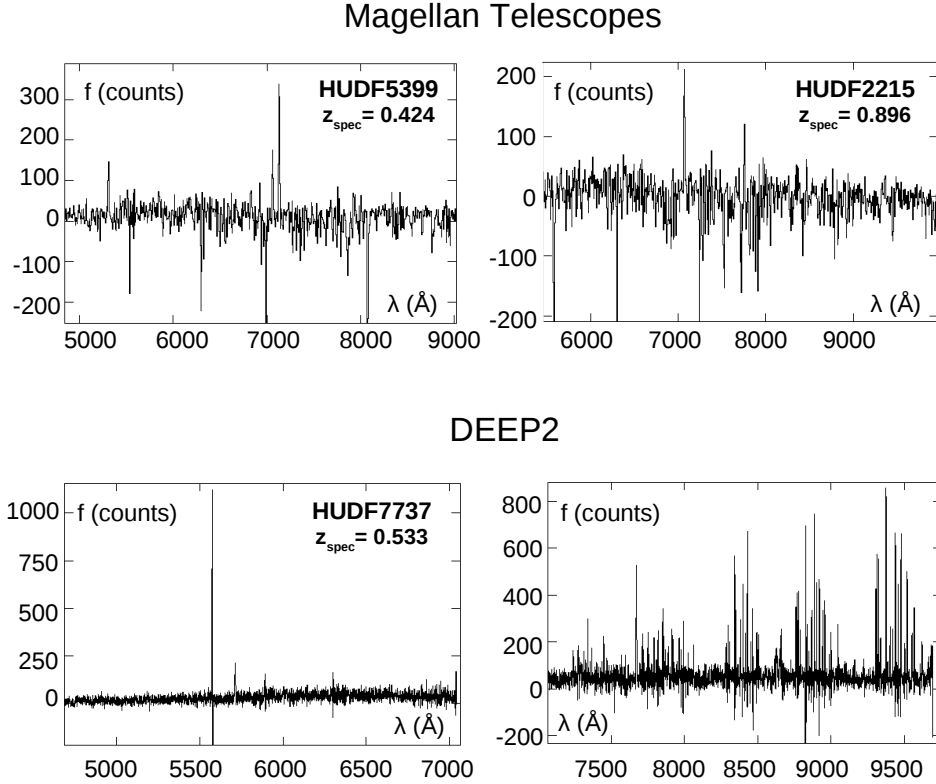


Figure 2: Spectra corresponding to some of the BCDs showed in Fig. 1 . DEEP2 spectrum is divided into two wavelength ranges.

and $10^{10} M_{\odot}$. We must take into account that these values could be underestimating the real masses due to the fact that the emission lines we measure are only related to a star burst component of the object, and not to the underlying stellar population. However, some studies have pointed out that this methodology is applicable to these less evolved objects [15]. A summary of the spectral properties of the BCDs appears in Table 1.

5 General properties and conclusions

We completed our study using the data base RAINBOW [13, 1], to fit the photometry of the objects to a Spectral Energy Distribution (SED), and then, estimate star formation rates and masses. In Fig. 3 (right) we present the specific star formation rate derived from synthetic UV luminosity over which we have applied an extinction correction [11, 10, 3], and compare it to the specific star formation rate derived from $H\alpha$ luminosity of the local star-forming

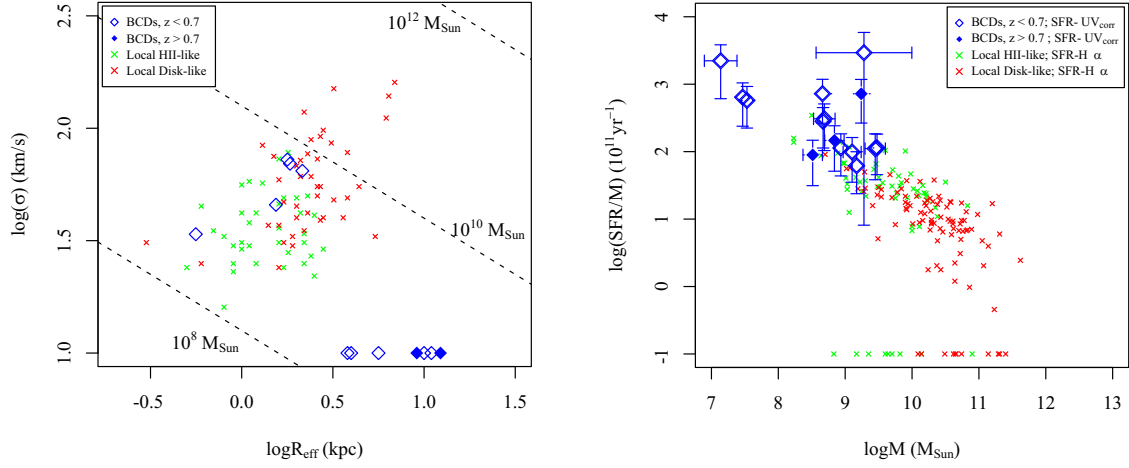


Figure 3: *Left*: velocity widths of the selected BCDs and local star-forming galaxies. Dashed lines indicate galaxy dynamical masses in solar units. *Right*: stellar mass in M_{\odot} vs. star formation rate per unit mass in yr^{-1} normalized to $10^{11} M_{\odot}$ for BCDs and local star-forming galaxies.

galaxies (UCM Survey [4]). We found that specific star formation rates of BCDs are on average 10 times greater than star-forming galaxies due to their 10 times smaller masses.

Attending to the properties identified we can classify the objects of the sample into three different groups: BCD-like galaxies, compact vigorous star-forming and low metallicity objects; irregular galaxies, that present similar but eased characteristics and higher masses by a factor ~ 10 ; and disk-like galaxies, characterized by the highest masses of the sample ($M \sim 10^{9.5} M_{\odot}$) and the lowest contribution of the star burst to the total luminosity of the object, that usually show morphological features such as arms and even bars. Finally, we identify an interacting object.

References

- [1] Barro, G., et al. 2011, in preparation
- [2] Beckwith, S. V. W., et al. 2006, AJ, 132, 1729
- [3] Calzetti, D. 2001, PASP, 113, 1449.
- [4] Gallego, J., et al. 1996, A&AS, 120, 323
- [5] Gil de Paz, A., et al. 2003, ApJS, 147, 29
- [6] Gil de Paz, A., et al. 2011, in preparation
- [7] Guzmán, R., et al. 1997, ApJ, 489, 559

Table 1: Properties of the sample of BCDs

Object	z_{spec}^a	$M_{B,0}^b$	$(B - V)_0^c$	r_{eff}^d	σ^e	$\text{EW}_{\text{rest},[\text{OII}]}^f$
HUDF0703	0.705†	-17.81	0.32	1.09	–	50 ± 9
HUDF0704	0.735†	-17.32	0.33	0.96	–	278 ± 115
HUDF1000	0.214‡	-16.36	0.28	1.00	–	–
HUDF2063	0.667‡	-18.14	0.46	1.54	46	34 ± 4
HUDF2215	0.896†	-18.30	0.25	2.52	–	171 ± 64
HUDF2998	0.605‡	-18.29	0.43	1.84	70	166 ± 45
HUDF3203	0.340§	-18.44	0.53	2.11	–	–
HUDF3445	0.434‡	-17.88	0.32	2.33	–	–
HUDF4825	0.337‡	-16.49	0.49	0.56	34	–
HUDF5399	0.424†	-16.09	0.38	0.60	–	98 ± 20
HUDF5620	0.212§	-16.32	0.27	1.04	–	–
HUDF6893	0.431†	-15.78	0.36	0.75	–	93 ± 28
HUDF7452	0.669‡	-18.02	0.35	2.15	65	54 ± 7
HUDF7737	0.533‡	-17.79	0.41	1.78	73	36 ± 5
HUDF9088	0.533†	-16.38	0.32	0.58	–	56 ± 18

^a †Spectroscopic redshift obtained by [6]; ‡Spectroscopic redshift from DEEP2; §Spectroscopic redshift from K20; \$Spectroscopic redshift from VVDS.

^b Absolute rest-frame B magnitude (mag in Vega scale).

^c Rest-frame $B - V$ color (mag in Vega scale).

^d Effective radius in kpc.

^e Velocity width in rest frame km s^{-1} (typical uncertainty $\sim 20\%$).

^f Equivalent width of $[\text{OII}]3727$ in \AA .

- [8] Jahnke, K., et al. 2004, PASP, 118, 1186
- [9] Kirby, E. N., et al. 2007, ApJ, 660, 62
- [10] Kong, X. 2004, A&A, 425, 417
- [11] Meurer, G. R., et al. 1999, ApJ, 521, 64
- [12] Mignoli, M., et al. 2005, A&A, 437, 883
- [13] Pérez-González, P. G., et al. 2008, ApJ, 675, 234
- [14] Phillips, A. C., et al. 1997, ApJ, 489, 543
- [15] Pisano, D. J., et al., 2001, AJ, 122, 1194
- [16] Thuan, T. X., & Martin, G. E. 1981, ApJ, 247, 823
- [17] Vanzella, E., et al. 2005, A&A, 434, 53
- [18] Vanzella, E., et al. 2006, A&A, 454, 423
- [19] Wolf, C., et al. 2004, A&A, 421, 913